Climatological Characterization of Puelche Winds down the Western Slope of the Extratropical Andes Mountains Using the NCEP Climate Forecast System Reanalysis

ALDO MONTECINOS[a]

Department of Geophysics, Center for Water Resources for Agriculture and Mining, University of Concepción, Concepción, Chile

RICARDO C. MUÑOZ

Department of Geophysics, University of Chile, Santiago, Chile

STEPHANIE OVIEDO, ANDRÉS MARTÍNEZ, AND VÍCTOR VILLAGRÁN

Department of Geophysics, University of Concepción, Concepción, Chile

(Manuscript received 26 August 2016, in final form 16 November 2016)

ABSTRACT

The existence of strong easterly winds down the western slope of the south-central Andes in Chile, locally known as Puelche winds, has been known by the meteorological community since at least the mid-twentieth century. However, this is the first time that a climatological characterization of them is presented. The analysis is based on 36 yr of daily CFSR–NCEP reanalyzed data, validated by surface weather observations. Puelche winds are present all year round. The main synoptic-scale forcing of Puelche winds in south-central Chile is the passage of cold anticyclonic systems across the Andes Mountains. As these systems progress into the South American continent, a zonal surface circulation crossing from Argentina (upslope) to Chile (downslope) develops. Unlike terral and raco, other foehnlike winds at subtropical latitudes in Chile, the Puelche winds are forced by both meridional and zonal pressure gradients. Presumably, the smaller altitude of the Andes Mountains south of 35°S allows the air crossing from east to west in response to the presence of the migratory high pressure system over Argentina. As in other places where foehnlike winds develop, the warming extends far from places where the Puelche is actually observed, that is, to the west of the Andes into the surface at the coastal and the central depression areas. This ''foehn clearance'' is the result of cloudless sky and drier atmosphere that would allow an increase in the solar radiation reaching the surface and a subsequent warming of the near-surface air. The foehn clearance also drives an enhanced nighttime cooling, especially on the days after the onset of the Puelche event.

1. Introduction

Mountains modify air motions from planetary to local scales (Barry 2008). The influence of mountains can be roughly categorized in two types: terrain-forced flows produced by the dynamic response of the atmosphere interacting with the topography, and the diurnal mountain winds produced by thermally driven circulations (Whiteman 2000). The daytime warming and nighttime cooling of slope surfaces in mountainous terrain or in the valley and surrounding plane system cause a diurnal cycle of upslope–up-valley (anabatic) and downslope–down-valley (katabatic) winds (Markowski and Richardson 2010). This surface wind diurnal cycle is the consequence of thermally induced pressure gradients between elevated surface and air at the same altitude over lower lands (Sturman 1987). In principle, the diurnal mountain winds do not need the presence of large-scale winds or the forcing of synoptic pressure gradients (Markowski and Richardson 2010), although they may be influenced by such large-scale factors (Whiteman and Doran 1993).

[a] Current affiliation: Departamento de Geofísica, Universidad de Chile, Chile.

Corresponding author e-mail: Aldo Montecinos, amonteci@dgeo.udec.cl

DOI: 10.1175/JAMC-D-16-0289.1

The kind of downslope winds studied in the present work is dynamically forced, corresponding to the terrain-forced flows described previously, where stability and speed of the air approaching to a barrier and the topographic characteristics determine the wind behavior (Whiteman 2000). These mountain winds are usually observed at the lee side of large and minor mountain ranges and are typically associated with warm and dry air (e.g., Brinkmann 1971; WMO 1992). Their presence has been reported in all major mountains of the planet and are called foehn in the Alps, chinook in the Rocky Mountains, germish in the southwestern part of the Caspian Sea, kachchan in Ceylon, Santa Ana in southern California, berg wind in South Africa, nor'wester in New Zealand, and zonda in Argentina, among many others.

Brinkmann (1971) summarized the early ideas that explained, since the mid-nineteenth century, the warm and dry characteristics of these descending winds: advection from drier and warmer zones, latent heat release and precipitation on the windward side of the mountain, adiabatic warming by compression in the leeward side, large-amplitude lee waves, and hydraulic supercritical flow. Nowadays, it is well established that the characteristic dryness and warming of the descending air is the product of adiabatic compression (e.g., Whiteman 2000). However, the downslope acceleration seems to be the result of processes that depend on the particular topographic characteristics of the barrier and the thermodynamic and dynamic state of the air approaching it. In the definition adopted by the WMO (1992), the speed is not an attribute of downslope winds, although it is used to characterize them in several works because of its importance for explaining the related impacts (e.g., McGowan and Sturman 1996; Raphael 2003; Gaffin 2007). According to Quaile (2001), wind speed decreases away from the mountain. In the European Alps, the foehn winds are perceived only as a temperature increase and a relative humidity decrease at distances up to 50 km downstream, while temperature rises can even be observed 100 km away (Quaile 2001). Hoinka (1985) defined as "foehn clearance" those events characterized by warm and dry air without increased wind speeds in the Alps. He found that maximum wind speeds are reduced by 60% at 70 km from the mountain. Interestingly, some foehn clearance events are easily identified from satellite observations by broad gaps in cloud cover in the lee of the Alps and the Rocky mountains.

In South America, zonda is a foehnlike wind that has received much attention (see location in Fig. 1a). It is characterized by strong, warm, very dry descending air along the eastern slopes of the Andes Mountains in west-central Argentina (30°–34°S), with more frequent occurrences during winter and spring seasons (Norte 1988, 2015). Seluchi et al. (2003) studied three typical zonda episodes during August 1999. The heating observed was about 10°–15°C in few hours, while the dewpoint temperature decreased in the same time interval by 15°–20°C, with wind gusts larger than 20 m s^{-1} at the surface. The synoptic configuration that forces the zonda is a surface cold front over Argentina, the associated low pressure system over the South Atlantic (~50°S), a 500-hPa leading trough and its related jet streak over the Andes summits at around 32°S, and high sea level pressure in Chile at the same latitudes (Seluchi et al. 2003; Norte et al. 2008). This configuration increases the cross-range pressure gradient and it can be used as a predictor of zonda (Norte 1988). Indeed, the zonda wind intensity is highly related to the surface pressure difference between San Juan (~31.5°S, ~68.5°W) in Argentina and La Serena (~30°S, ~71.5°W) in Chile (Seluchi et al. 2003).

In central Chile, foehnlike winds are locally known as terral in the Elqui Valley near La Serena (~30°S) and raco in the San José de Maipo Valley, south of Santiago (~33°S). However, in south-central Chile, a region of 600 km of latitudinal extension, these episodes are generically known as Puelche, without association with specific valleys (see locations in Fig. 1a). Rutllant and Garreaud (2004) studied the raco winds, showing that katabatic–nocturnal flows down the narrow Andean valleys within the western slope of the subtropical Andes are episodically enhanced by easterly downslope winds. About 80% of raco episodes occur as a warm ridge at midlevel is situated just to the west of the subtropical Andes. Similarly, 65% of terral events are driven by the same synoptic forcing (Montes et al. 2016). Under these circumstances, the typical equatorward pressure gradient along the coast of central Chile is reversed by a high pressure system crossing the Andes in southern Chile. The imposed meridional pressure gradient forces a geostrophic response leading to a regional-scale, low-level easterly (offshore) flow developing at the coast and inland, and triggering and sustaining most of the strong downslope raco and terral events. The remaining 20% (35%) of raco (terral) events are mainly characterized by a prefrontal condition ahead of a trough driving northwesterly 500-hPa winds.

In south-central Chile, a region of 600 km of latitudinal extension, episodes of intense easterly winds are generically known as Puelche, without association with specific valleys. Puelche is a native word for "east men," referring to the people living on the eastern side of the Andes (Argentina). At these latitudes the distance from the Pacific coastline to the Andes foothills (~200 m of altitude) is just about 100–150 km. From west to east, the topography can be divided in four distinctive geographical zones: the coastal plain with heights below 100 m MSL,

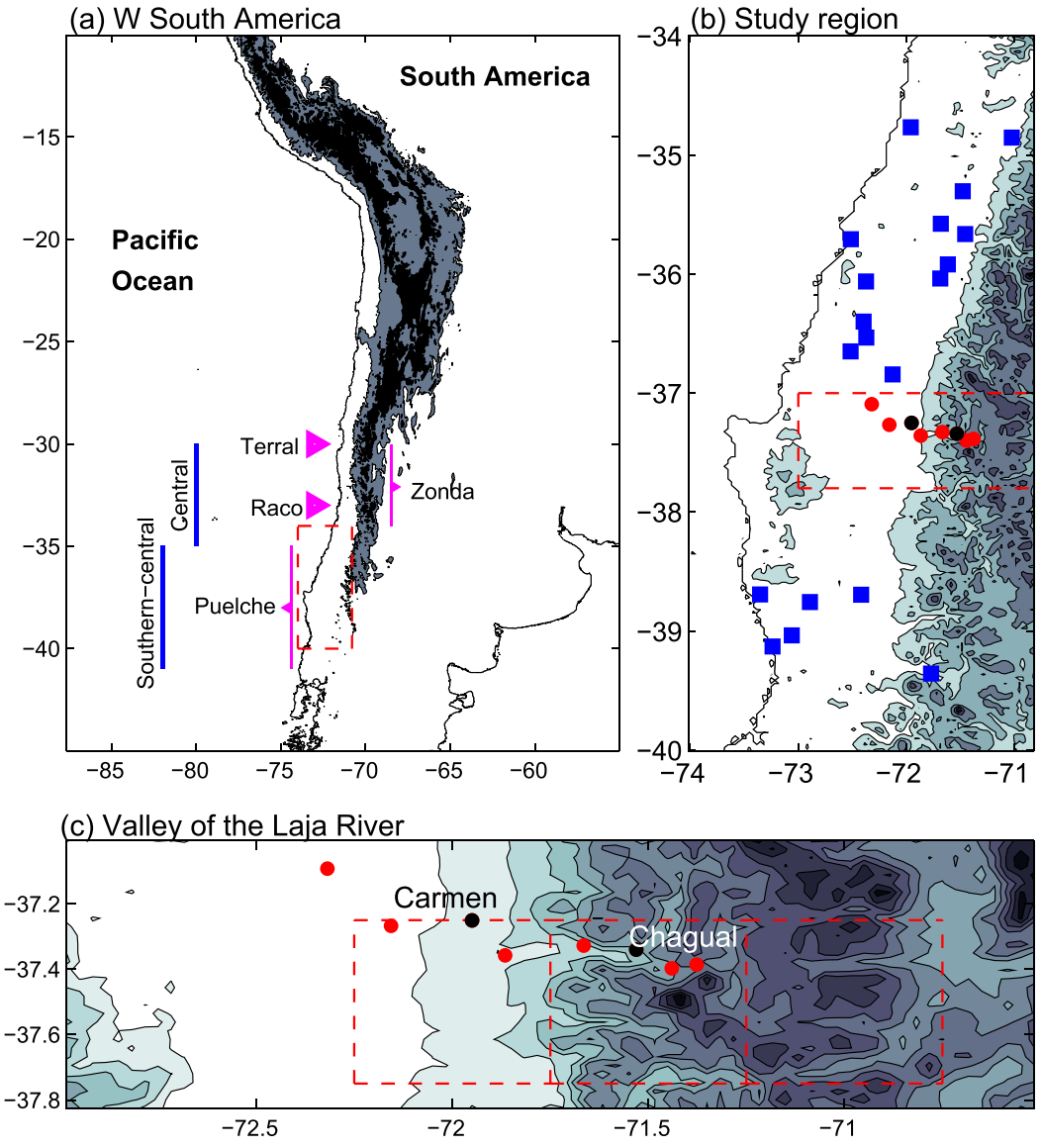

FIG. 1. (a) Location of the study region in western South America (red dashed rectangle). Areas with regional foehnlike wind systems are identified in pink. (b) Location of weather stations with daily data in the following periods: January 2009–December 2013 (blue squares) and February 2014–February 2015 (red and black circles). (c) Location of weather stations along the valley of the Laja River. Red dashed rectangles denote the CFSR–NCEP grids used for validation and identification of Puelche events (see text for details). Topography is shaded every 2000, 500, and 250 m MSL in (a), (b), and (c), respectively. The western (eastern) black circle in (b) corresponds to the Carmen (Chagual) weather station, also identified in (c).

the coastal range that rises up to 700–1500 m MSL interrupted only by rivers, the central depression with heights between 100 and 300 m MSL, and the Andes Mountains ranging from 4000 m MSL at 35°S to 2000 m MSL at 37°S. The surface atmospheric circulation in the eastern South Pacific, and along coastal areas, has received much attention because of its importance for the coastal upwelling phenomenon (e.g., Strub et al. 1998; Rutllant et al. 2004; Garreaud and Falvey 2009; Montecinos and Gomez 2010). In south-central Chile the wind seasonality is related to the seasonal north–south migration of the South Pacific subtropical anticyclone (Fuenzalida 1982). During austral spring and summer the South Pacific subtropical anticyclone reaches its southernmost position, explaining the prevailing equatorward alongshore winds and the related upwelling season. In winter, when the South Pacific

subtropical anticyclone progresses equatorward, midlatitude weather systems experience their northernmost position, alternating poleward and equatorward winds along the coast. Muñoz and Garreaud (2005) and Garreaud and Muñoz (2005) described an equatorward low-level coastal jet off central Chile forced by meridional pressure gradients, only semi-geostrophically balanced because of the influence of the coastal topography, associated with the passage of surface high pressure systems at midlatitudes.

Interestingly, Puelche was mentioned by Glenn (1961), and afterward by other authors (e.g., Brinkmann 1971; Quaile 2001; Drechsel and Mayr 2008), as a typical foehnlike wind in the Andes, although no specific work had been done on this local wind. Puelche is referred to as an "easterly foehn" wind of the Andes by Glenn (1961), who took this statement from the *Glossary of Meteorology*. The aim of the present paper is thus to characterize, for the first time, the foehnlike wind called Puelche in south-central Chile. The paper is organized as follows: Section 2 describes the data and methodologies. The results and discussion are presented in section 3. Finally, section 4 contains the main conclusions of this work.

2. Data and methodology

a. Study region and data

The analysis of the occurrence of Puelche winds in south-central Chile (35°–41°S) is mainly based on observed and gridded daily values of meteorological variables. The observations comprise two datasets. The first is a compilation of data from 19 surface automatic weather stations (AWSs) spanning different time periods between years 2009 and 2013 and covering the latitudinal band 34.5°–39.5°S (blue squares in Fig. 1b). These data are used in section 3c to show the general impact of Puelche winds on surface temperature and winds over the central depression region of the study domain. The second observational dataset corresponds to a network of eight AWSs operating since February 2014 in the valley of the Laja River at different altitudes from the middle of the central depression (150 m MSL) to the head of the valley (1400 m MSL) around 37.3°S (red and black circles in Fig. 1b). This meteorological network provides a unique source of data in the western slope of the Andes in south-central Chile and is used in section 2b to validate the gridded dataset described next.

The gridded dataset, the Climate Forecast System Reanalysis (CFSR) of the National Centers for Environmental Prediction (NCEP), consists of a high-resolution global reanalysis, with a coupled atmosphere–ocean–land surface–sea ice system, which merges observations and model data (Saha et al. 2010, 2014). The CFSR–NCEP reanalysis has a spatial resolution of 0.5° × 0.5°, every 6 h, from January 1979 to February 2015. Daily averages were computed considering gridded values at 0600, 1200, 1800, and 0000 UTC. As will be shown in the results section, the grid point at 37.5°S, 71.5°W (Fig. 1c) of the reanalysis represents well the zonal wind variability in the middle of south-central Chile. The time series of the near-surface zonal wind component (sigma 0.995 level) at this grid point is subsequently used to characterize the Puelche wind for the 36 yr of the CFSR–NCEP reanalysis.

Finally, to evaluate the association with Puelche events and regional cloudiness, 1-km-resolution visible GOES imagery has been analyzed. In particular, the albedo-based algorithm described by Molina (2012) and Rondanelli et al. (2015) was used to discriminate between clear and cloudy pixels in the continental region between 34° and 40°S, considering GOES scans closest to hours 0900, 1200, and 1500 local time for each day in the period 2004–14. Averaged clear-sky fractions were computed for seasonal periods as well as for the subset corresponding to the first days (day +1) of Puelche events.

To extract the annual cycle and focus on the synoptic variability of winds, two different approaches are used. For the observations, the daily anomaly is defined by removing the week-mean value from each day and then moving to the following week until the entire period is completed. For gridded time series, on the other hand, the long-term (full period) average for each day, smoothed with a simple moving average of 11 days, defines the annual cycle that is subsequently removed from daily values to calculate daily anomalies.

b. Validation

Because of the scarcity of long-term meteorological records over the western slope of the Andes Mountains, the climatological characterization of the downslope Andean winds in south-central Chile is mainly based on gridded data. The CFSR–NCEP reanalysis has already been used in the literature to characterize near-surface wind variability: to force wind-wave models (e.g., Chawla et al. 2013; Stopa and Cheung 2014), to study the influence of high-resolution wind stress on forcing near-inertial ocean motions (Rimac et al. 2013), to study the low-frequency fluctuations of low-level winds for power generation in China (Yu et al. 2016), to study sea level extremes associated with storm surges (Zhang and Sheng 2013), and to perform a synoptic climatology analysis of the near-surface wind in the southeastern Pacific (Rahn and Garreaud 2014), among several other studies.

The comparison between observations and CFSR–NCEP reanalysis is based mainly on the correlation coefficient, an index of the phase relation between two time series,

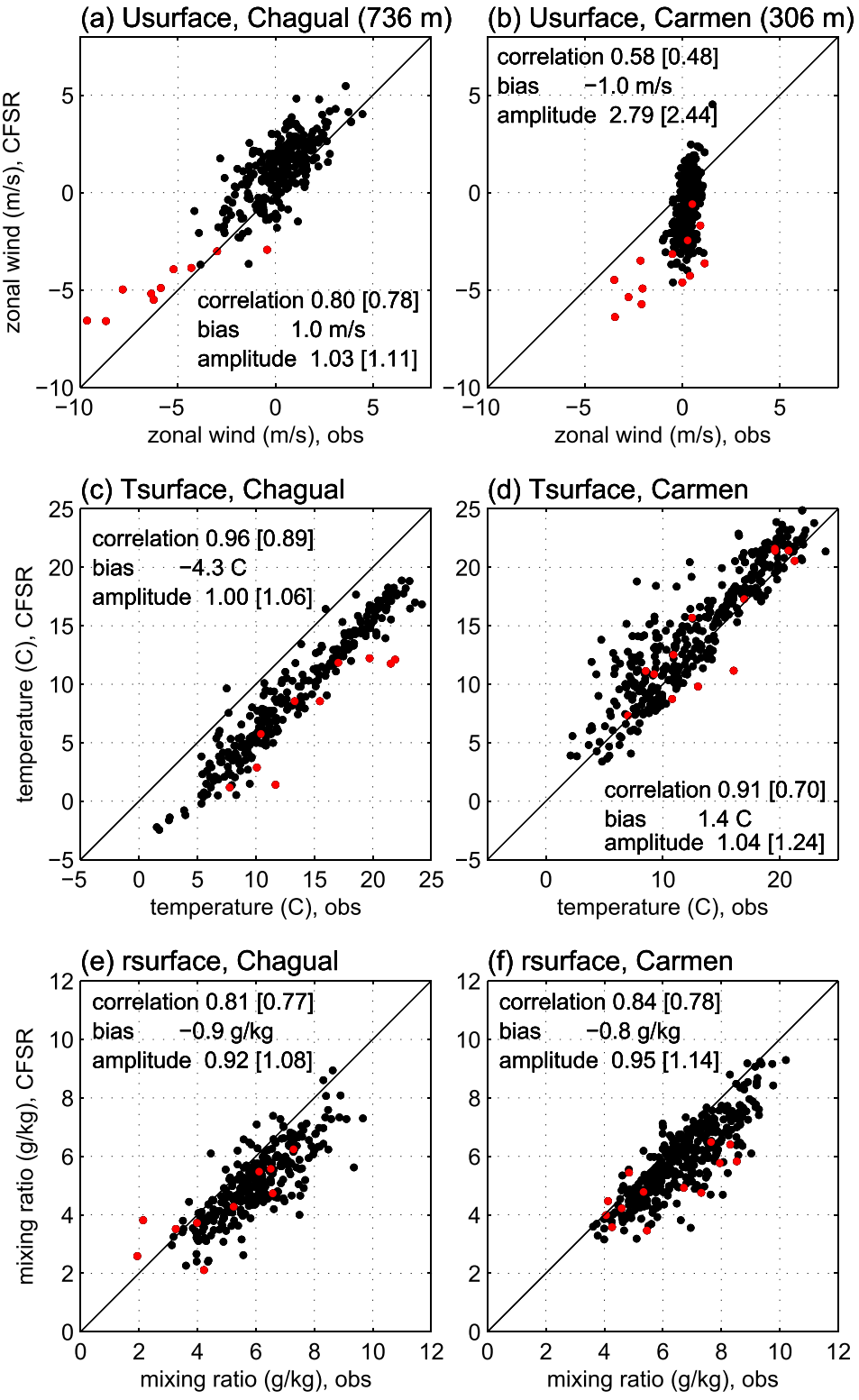

FIG. 2. Scatterplots of absolute values of (a),(b) zonal wind component ($m\,s^{-1}$); (c),(d) temperature (°C); and (e),(f) water vapor mixing ratio ($g\,kg^{-1}$) between observations (horizontal axis) and the nearest CFSR grid point at the sigma 0.995 level (vertical axis) for (left) Chagual and (right) Carmen. The correlation, bias (mean difference of CFSR − observation), and amplitude (standard deviation ratio of CFSR/observation) is shown for every scatterplot, using absolute and anomaly (in brackets) values. See text for definitions. The 1:1 line is shown for reference. Red circles show Puelche events according to criteria described in section 2c and Fig. 3 (below).

but also on the difference between CFSR and observed averages (bias), and the ratio between CFSR and observed standard deviations (amplitude). This comparison is made using two weather stations: Chagual (736 m MSL) and Carmen (306 m MSL), identified in Fig. 1c. They are considered representative of the center of the Laja transverse valley (Chagual) and a point off its mouth to the west (Carmen). These weather stations were compared with CFSR grids along 37.5°S centered at 71.5°W (1375 m MSL) and 72°W (408 m MSL), respectively (Fig. 1c). The variables compared in Fig. 2 are zonal wind, temperature, and water vapor mixing ratio. The verification statistics were computed using the 13-month period from February 2014 to February 2015 (384 days for Carmen and 284 days for Chagual). To take into account the effect of the seasonal cycle signal, correlations and amplitudes were calculated using full values as well as anomaly values, as defined at the end of section 2a.

Figures 2a and 2b show that larger correlations between CFSR and observed zonal winds are found at the higher site (Chagual, $r \sim 0.8$) as compared with the lower site (Carmen, $r \sim 0.5$) when daily anomaly values are considered. At Carmen, the observed variability of zonal winds is much reduced as compared with that of the corresponding CFSR grid point, as quantified by an amplitude of about 2.5. This large overestimation of the variance by the reanalysis is probably indicating that the actual topographic sheltering of Carmen station located at the surface in the central depression cannot be captured by the 50-km-resolution gridded data. It is noteworthy, however, that the special events of strong easterly winds in the observations are well captured by the reanalysis at both sites. Correlations of temperatures (Figs. 2c,d), on the other hand, show at the two sites higher values as compared with those of zonal winds ($r \sim 0.9$ at Chagual and $r \sim 0.7$ at Carmen). In terms of biases, at Chagual there exists a small positive (larger negative) bias for the zonal wind (temperature), which is consistent with the higher altitude (1375 m MSL) of the grid point as compared with the station (736 m MSL). At Carmen, the bias in temperature is reversed although it is only 1.4°C, the difference in altitudes between grid point and station being smaller. For water vapor mixing ratio (Figs. 2e,f) the comparison at the center of the Laja Valley and off the valley mouth to the west is similar. Correlations based on daily anomalies are just below 0.8 and there is a small overestimation of the variance. Also, there exists a negative bias in the CFSR data of about $-1\ \mathrm{g\,kg^{-1}}$. The general conclusion drawn from Fig. 2 is that the CFSR–NCEP reanalysis does a reasonable job in reproducing the variability of zonal winds, temperature, and water vapor mixing ratio in the study region, with some biases explained by its horizontal and vertical resolution. As could be expected, the reanalysis has problems in reproducing the variability of the generally weak surface winds in the central depression, but as noted above, it still captures the special events of intensified easterly winds that are the focus of the current analysis.

c. *Classification procedure*

Brinkmann (1971) pointed out the difficulties in formulating a general objective definition of foehnlike winds due to differences in location and seasonality. Foehn events can be characterized by simultaneous and abrupt changes in temperature, humidity (relative, equivalent, or dewpoint temperature), and surface winds flowing from the mountains. Identifying when such foehnlike winds begin and end is a difficult task that needs clearly defined criteria to be reproducible. Recently, suitable automated classification algorithms have been proposed based on hourly observed values (e.g., Plavcan et al. 2014).

In Chile at ~33°S, raco wind episodes during winter were simply defined by Rutllant and Garreaud (2004) as consecutive days in which the hourly averaged down-valley wind speeds exceeded a threshold of $5\ \mathrm{m\,s^{-1}}$ between 0400 and 0700 local time. In their study of terral episodes at ~30°S, Montes et al. (2016) defined them as cases with easterly winds with speeds $> 2\ \mathrm{m\,s^{-1}}$, temperature > 11°C, and relative humidity $< 30\%$, between 0100 and 0700 local time.

Because of the unavailability of long-term records of hourly observations in our region of interest, the definition methodology proposed by Plavcan et al. (2014) is adapted here to be used based upon the CFSR–NCEP gridded data. They pointed out that during foehnlike winds the magnitude of the potential temperature difference ($\Delta\theta$) between two sites located at different altitudes along a valley is reduced. Contrarily, strong katabatic winds due to nocturnal radiative cooling lead to stable stratification, that is, larger and positive $\Delta\theta$. Thus, to classify foehnlike winds in south-central Chile there are two conditions to be met: zonal wind must be negative and $\Delta\theta$ must be reduced or close to zero.

Figure 3 shows scatter diagrams (Figs. 3a,c) of the variables used in the classification procedure of Puelche events: $\Delta\theta$ between grid points 37.5°S, 71.0°W (1659 m MSL) and 37.5°S, 71.5°W (1375 m MSL), and zonal wind U at 37.5°S, 71.5°W (grid point in comparison with Chagual station in Fig. 2), for summer and winter conditions. In summer (Fig. 3a), while the vast majority of cases consist of westerly winds ($U > 0$) with stable stratification ($\Delta\theta$ between 2° and 4°C), a well-defined tail in the point cloud is apparent, with easterly winds ($U < 0$)

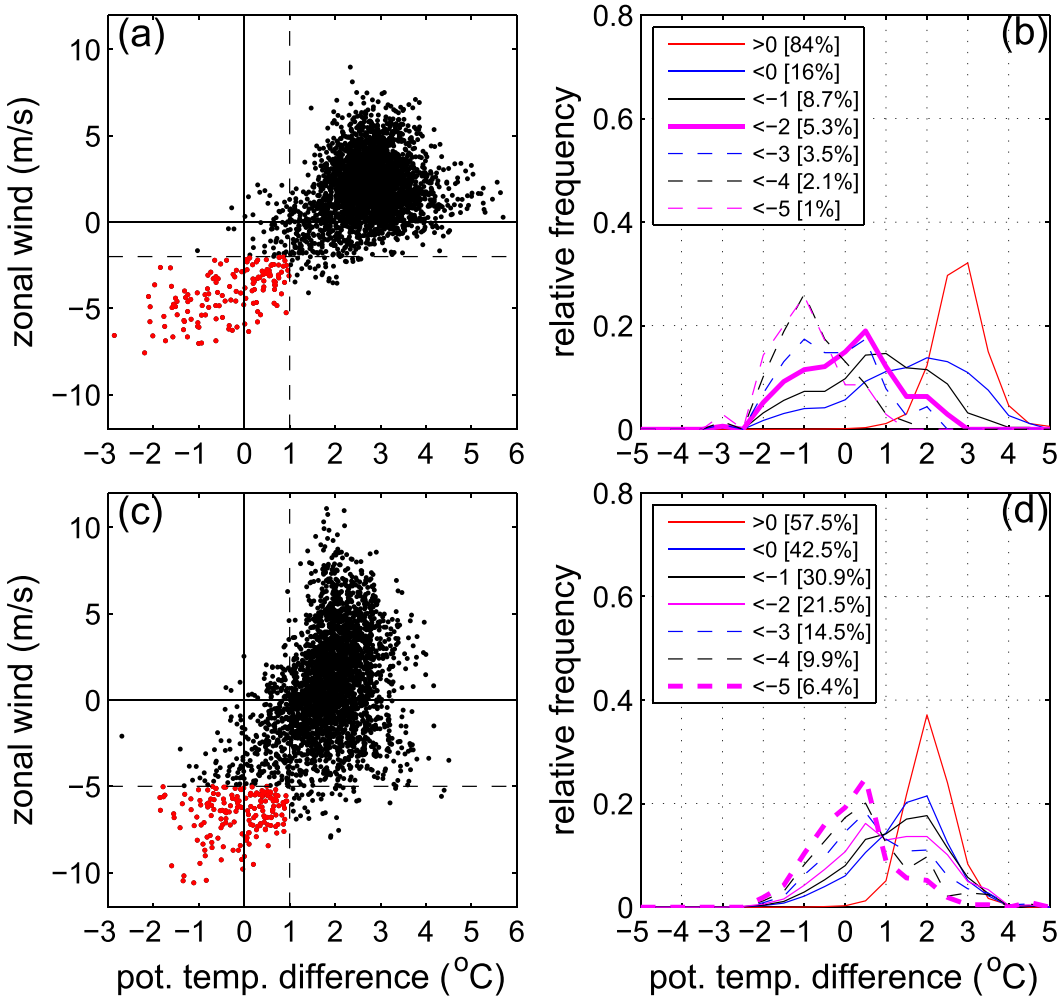

FIG. 3. (a) Scatterplot of daily potential temperature difference ($\Delta\theta$) between the summit (37.5°S, 71°W) and the slope (37.5°S, 71.5°W) CFSR grid points and daily zonal wind (U) at the slope (37.5°S, 71.5°W) for summer days between 1979 and 2015. Red dots indicate days chosen as Puelche events, i.e., $U < -2\,\mathrm{m\,s^{-1}}$ and $\Delta\theta < 1$°C. (b) Relative frequency distribution of $\Delta\theta$ depending on different zonal wind thresholds identified by the different solid and dashed colored lines. The thick line shows the chosen criteria for selecting Puelche events. (c) As in (a), but for winter days between 1979 and 2014, with $U < -5\,\mathrm{m\,s^{-1}}$ and $\Delta\theta < 1$°C. (d) As in (b), but for winter days. Values in brackets show the conditional probability (%) of $\Delta\theta$ when U is above or below of different thresholds.

and reduced or even negative values of $\Delta\theta$. A similar though less marked point distribution is appreciated in winter cases (Fig. 3c). A complementary way of visualizing the (U, $\Delta\theta$) relationship is presented in Figs. 3b and 3d, where the relative frequency distributions of $\Delta\theta$ conditional to different zonal wind thresholds are shown. As the U threshold moves to lower values, the $\Delta\theta$ distributions shift to more negative values. Similar behavior is observed for fall and spring seasons (not shown). In our classification procedure, the threshold for the zonal wind is chosen as the value at which the conditional $\Delta\theta$ distributions are centered around zero (bold distribution lines in Figs. 3b,d). With such criterion, the zonal wind thresholds are $-2\,\mathrm{m\,s^{-1}}$ in summer, $-3\,\mathrm{m\,s^{-1}}$ in fall, $-5\,\mathrm{m\,s^{-1}}$ in winter, and $-5\,\mathrm{m\,s^{-1}}$ in the spring season. As seen in Figs. 3a and 3b, however, the conditional $\Delta\theta$ distributions with these thresholds still show a right-hand tail that includes cases with significant stability. The latter are removed by adding a condition that $\Delta\theta$ must be lower than 1°C.

An indirect and independent testing of the quality of the classification procedure is shown in Fig. 4. Daily zonal winds and relative humidity observed at Chagual and Carmen (black circles in Fig. 1c), are depicted along with the days chosen as Puelche events with our CFSR-based criterion. For these variables, a foehnlike wind should be characterized by an increase in the easterly (downslope) wind speed together with a decrease in the

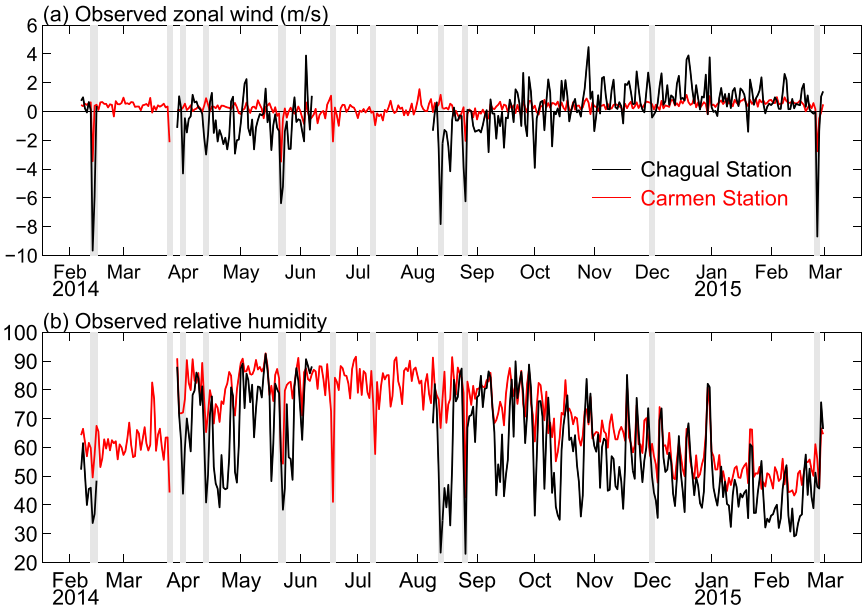

FIG. 4. Observed time series of (a) zonal wind ($m\,s^{-1}$) and (b) relative humidity (%) at the weather stations of Chagual (black lines) and Carmen (red lines). Vertical gray lines exhibit Puelche events identified with the criteria shown in Fig. 3.

relative humidity. With few exceptions, most of the chosen events clearly correspond to Puelche episodes actually observed in the valley of the Laja River. In spite of gaps at Chagual, most of Puelche events coincide with easterly speeds larger than $4\,m\,s^{-1}$ and a reduction of the relative humidity below 50%, especially distinctive in summer, fall and winter of 2014. At Carmen, located to the west of the Laja valley mouth, with few exceptions there is no evidence of strong easterlies during Puelche episodes but there is a clear decrease in the relative humidity.

d. *Analysis procedure*

According to the classification procedure described above, Puelche events occur all year round in south-central Chile, with a relative maximum (minimum) in fall (spring). There is, on average, one event per month, lasting for one day (~67%), two days (~22%), three days (~10%), and four days (~1%). For a comprehensive picture of the evolution of Puelche episodes at 37.5°S, we focused the subsequent analysis on events with durations of two days (day 0 and day +1, hereafter), and show results for summer and winter seasons. In general, the composite analysis for events lasting 1 day shows similar results (not shown). Results for the transitional seasons of fall and spring are generally intermediate of those presented here for the extremes of the annual cycle.

Compositing analysis is performed to characterize the synoptic-scale circulation associated with the occurrence of Puelche episodes and the related atmospheric anomalies at regional scale. The statistical significance is evaluated by Monte Carlo tests at 95% of confidence level (von Storch and Zwiers 1999).

3. Results and discussion

a. *Synoptic forcing*

The compositing analysis of the synoptic forcing is based on sea level pressure (SLP) and geopotential height at 500 hPa (Fig. 5), for the previous day (day −1) of the Puelche onset, and for day 0 and day +1. The synoptic configuration for all seasons is similar. During day 0 the main synoptic driver for the occurrence of Puelche episodes in south-central Chile is the passage of a cold migratory anticyclonic system crossing Chile–Argentina at midlatitudes with an upper-level ridge to the west of the Andes Mountains. The eastward displacement of this high pressure system is better seen in the SLP anomaly fields. On day −1, the high pressure center is located off Chile at 50°S and 85°–80°W along with a ridge aloft. During day 0, the system is centered at 50°S and 70°–75°W over Patagonia with a northward displacement over Argentina. In the upper levels, southwesterly winds are observed over south-central Chile, between a ridge to the west and a trough to the east of the Andes. By day +1, the migratory anticyclone is totally displaced along Argentina while the

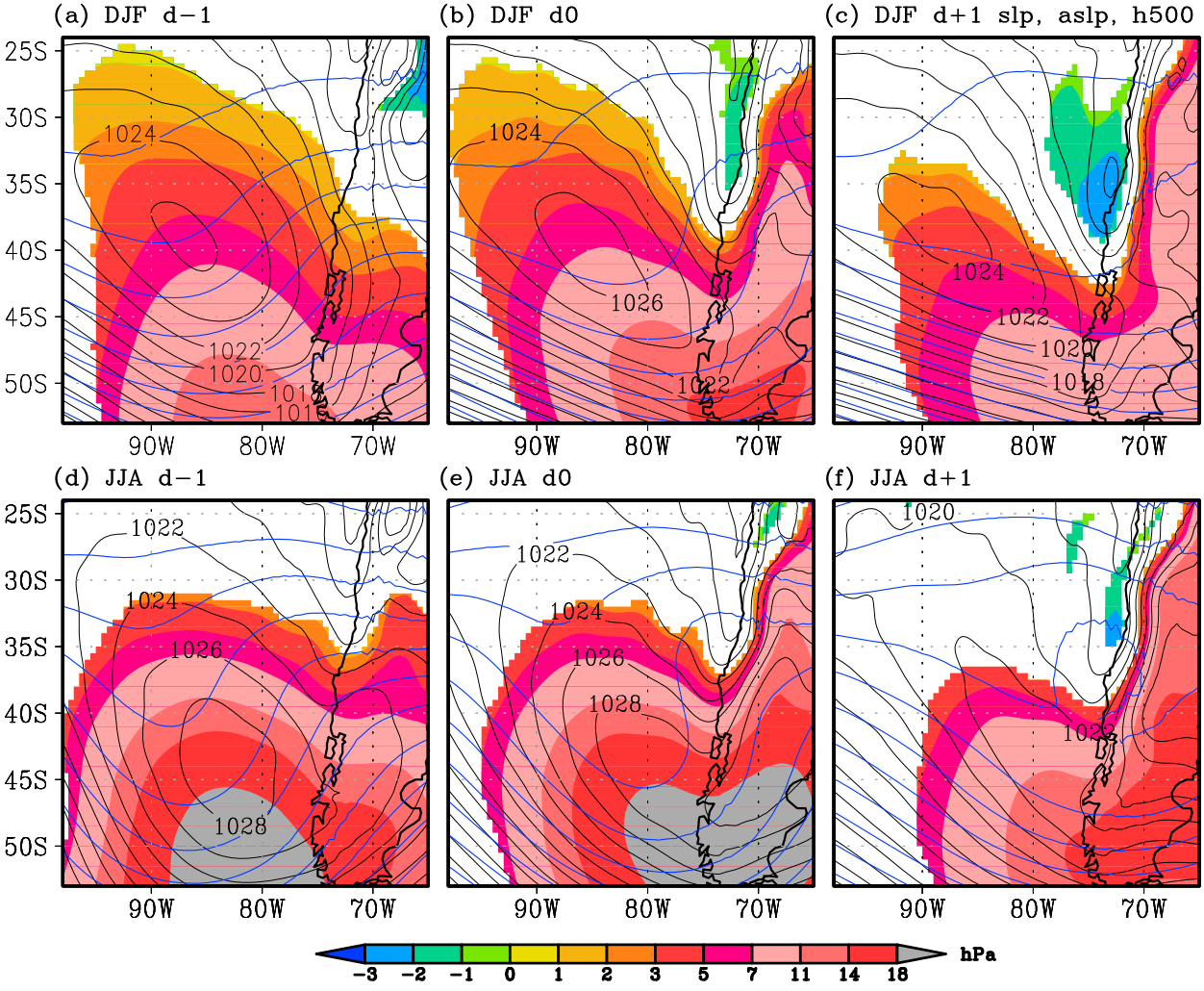

FIG. 5. Composite of the CFSR SLP absolute (black lines) and anomaly (color shades) values and the CFSR geopotential height at 500 hPa (blue lines every 40 m) (a),(d) one day before; (b),(e) the first day of; and (c),(f) the second day of Puelche events that last two days. The composites are shown for summer in (a)–(c) and winter in (d)–(f). Anomaly composites are shown when values are significant at 95% of confidence based on a Monte Carlo test. Composite averages are based on absolute SLP and 500-hPa geopotential height, and anomaly values for SLP in the period January 1979–February 2015.

ridge axis has reached the continent. From day 0 to day +1, a coastal low along the Chilean coast moves southward and intensifies, reaching the minimum SLP at about 35°S. It is worth noting that in 15% (35%) of Puelche events during summer (winter), along with the migratory anticyclone in surface and the upper-level ridge approaching the continent there is a cutoff low centered at about 35°S between 80° and 75°W (not shown).

The first indications of the importance of these synoptic configurations in forcing subsynoptic and mesoscale weather phenomena in Chile were related to the occurrence of coastal lows or troughs that in turn have been associated with air pollution episodes in the city of Santiago at ~33°S during winter (Rutllant and Garreaud 1995; Garreaud et al. 2002; Garreaud and Rutllant 2003). The meridional pressure gradient to the west of the Andes, within a zonal scale of about the Rossby radius of deformation (about 100 km to the west), forces a geostrophic (downslope) flow in north-central Chile that is responsible for the coastal trough development because of the adiabatic warming associated with the easterlies down the western slope of the Andes (Fig. 14 in Garreaud et al. 2002). Associated with the migratory anticyclone that triggers Puelche episodes in south-central Chile during all seasons (shown just for summer and winter in Fig. 5), we also note the development of coastal troughs along the coast that culminate at 35°S during day +1 (Figs. 5c,f).

To establish the meridional scale of Puelche events and the temporal wind behavior in the west-to-east

direction, a compositing analysis is made for zonal winds in the western slope, summit, and eastern slope of the Andes Mountains over a period encompassing 3 days before and 2 days after the occurrence of a two-day Puelche episode (Fig. 6). During summer, negative zonal winds develop in the meridional band 35°–41°S exclusively during the two days of the event. In the summit and eastern slope, easterly winds are also observed northward of 35°S during the development of the Puelche event. To the south of 41°S, however, only westerly winds are present during the Puelche event. During winter, which is closer to the fall and spring situations (not shown), the meridional scale of the easterly or downslope winds in the western flank of the Andes extends from 35° to 45°S, although with smaller easterly speeds south of 43°S. Unlike summer, easterly winds are noted the day before the onset of Puelche event in the latitudinal band 37°–41°S. In any case, stronger easterlies are visible during day 0 and day +1 between 37°S and 41°W. In the summit, the easterly component is restricted to the latitudinal band 35°–41°S during day 0 and day +1 of the episode. In the eastern Andean slope, the easterly wind is weaker in the latitudinal band 34°–40°S, while to the south it is positive (Fig. 6).

The absence of simultaneous easterlies to the north of 35°S while Puelche events develop, as seen in Fig. 6, suggests that terral and raco events in central Chile (30°–33°S), which take place mostly during winter, generally do not coincide with Puelche events in south-central Chile (35°–40°S). The simplest explanation is related to the latitudinal position of the migratory anticyclone. When the high pressure center crosses the Andes along 40°S, raco and terral episodes are forced in central Chile (Fig. 6 in Rutllant and Garreaud 2004; Fig. 6 in Montes et al. 2016). On the other hand, when the high pressure center moves eastward along 50°S in winter, Puelche events are forced in south-central Chile (Fig. 5).

Rutllant and Garreaud (2004) discussed the role of the cross-range pressure gradient, or zonal pressure gradient in the case of the subtropical-to-midlatitude Andes, in the forcing of raco events in central Chile (~33°S). Based on the differences of pressure at different heights between Mendoza radiosonde station (~33°S, Argentina) and Quintero (~33°S, Chile), it was shown that positive zonal pressure gradients are confined below 3000 m MSL (see Fig. 10a in Rutllant and Garreaud 2004), concluding that the cross-range pressure gradient is not forcing an east to west circulation near the surface, since the mean altitude of the Andes at these latitudes is near 5000 m MSL with few gaps with altitudes over 3500 m MSL. On the other hand, negative meridional pressure gradients, calculated as the difference between Quintero (~33°S) and Puerto Montt, Chile (~41.5°S), are confined below 1000 m MSL (see Fig. 10b in Rutllant and Garreaud 2004).

In south-central Chile, however, to the south of 35°S the mean altitude of the Andes drops from 4000 m to 2000 m MSL at 37°S. Under similar synoptic forcing, it is expected that the easterly winds flowing across the Andes from Argentina (upslope) to Chile (downslope) may be forced by both zonal and meridional pressure gradients, while the migratory anticyclone progresses from the coast of southern Chile into Argentina. Regarding this phenomenon, Fig. 7 shows the point-to-point correlation based on daily anomalies in the entire period 1979–2015 between the near-surface wind components and the surface pressure gradients. In south-central Chile, particularly in the western slope of the Andes south of 37°S, the meridional pressure gradient and the zonal wind have positive correlations on the order of 0.7, suggesting a geostrophic response of the zonal circulation (Fig. 7a). Additionally, south of 35°S there is a strong negative correlation between the zonal pressure gradient and the zonal wind on the order of −0.7, indicating that the zonal wind is also affected by the cross-range pressure difference (Fig. 7b).

For the near-surface meridional wind, the zonal pressure gradients exhibit geostrophic correlations larger than 0.9 over the ocean although decreasing to the north of 30°S (Fig. 7c). The strong and negative correlations between the meridional wind and the meridional pressure gradients off central Chile shown in Fig. 7d is consistent with the finding of Muñoz and Garreaud (2005) on the semigeostrophic balance supporting the low-level coastal jet in central Chile, which has also been recently corroborated by Rahn and Garreaud (2014). Interestingly, Fig. 7d shows that at these more southerly latitudes, the meridional wind–meridional pressure gradient relationship is also present over the land between the coast and the western slope of the Andes Mountains in south-central Chile, suggesting that the semigeostrophic balance may extend inland because of the blocking effect of the Andes.

b. *Regional circulation*

The composites of surface temperature anomalies and surface zonal and meridional wind components during day −1, day 0, and day +1, are shown in Fig. 8. Upper-level winds at 850 hPa and surface water vapor mixing ratio anomalies are shown in Fig. 9.

For summer, positive temperature anomalies (above 0.5°C) are observed during day 0 in south-central Chile, increasing up to 4°C during day +1 to the south of 37°S (Figs. 8a–c). Contrarily, during winter negative surface temperature anomalies are extensively present during day −1 and day 0 in most places over the coastal ocean

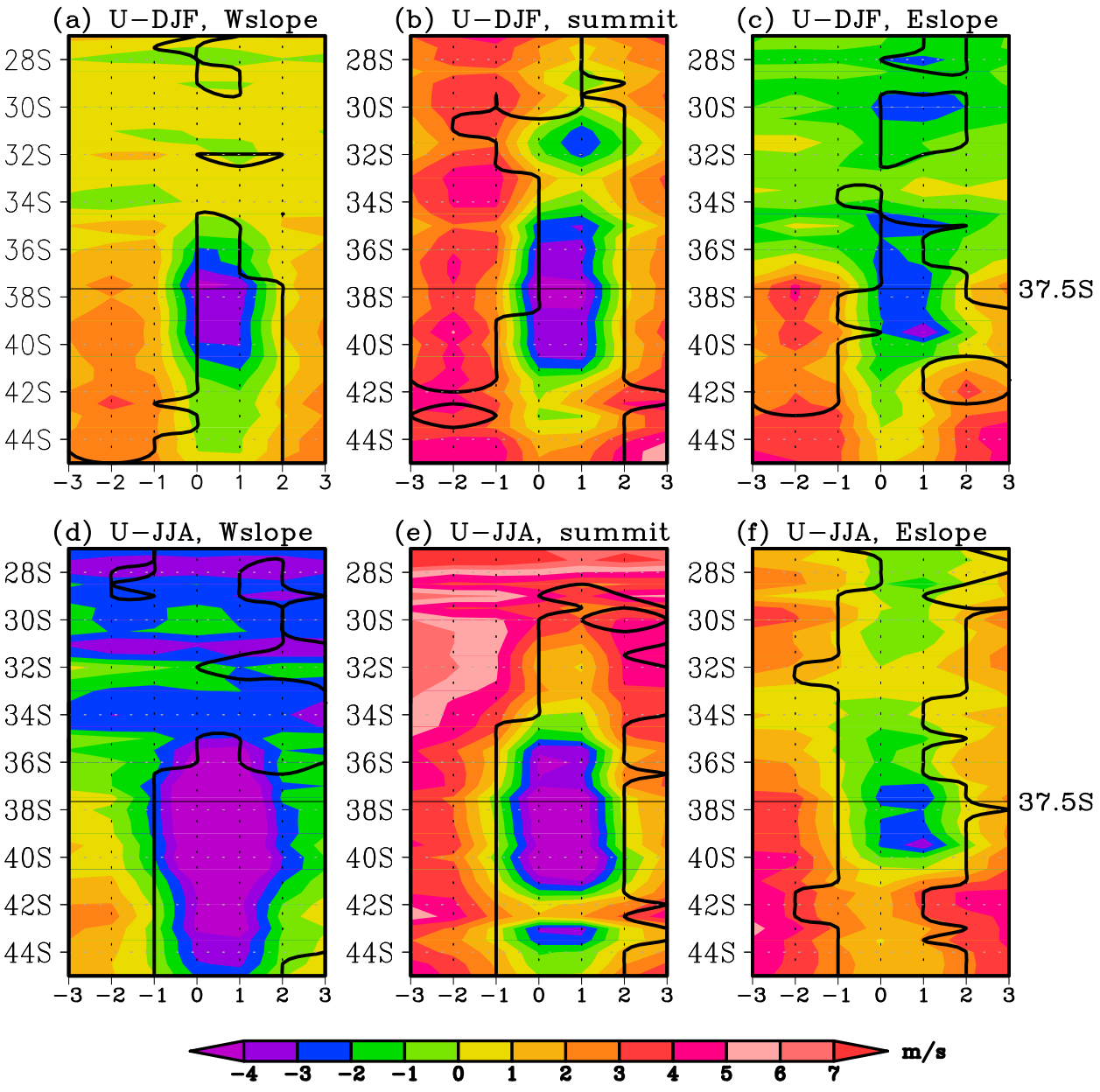

FIG. 6. Composite of the CFSR zonal wind ($m\,s^{-1}$, color shades) along (a),(d) the western slope; (b),(e) the summit; and (c),(f) the eastern slope of the Andes Mountains between 45° and 27°S (vertical axis) for Puelche events that last two days (0 and 1 in the horizontal axis). Black thick lines show statistical significance at 95% of confidence based on a Monte Carlo test. The horizontal axis shows from 3 days before the first day (−3, −2, and −1) and 2 days after the second day of the Puelche event (2 and 3). Composite averages are based on absolute zonal wind values in the period January 1979–February 2015.

at midlatitudes, and over Chile to the south of 37°S (Figs. 8d–f). By day +1, negative temperature anomalies decrease in the study region. Fall and spring seasons show a mixed pattern (not shown): surface temperature anomalies over 1°C are seen at day +1 south of 35°S in fall, while in spring negative anomalies are restricted to the region 37°–41°S during day 0. In Argentina, strong negative anomalies develop during day 0 and day +1 in all seasons. Though negative anomalies are noted during day 0 in south-central Chile during winter and spring, there is an evident warming during the development of the Puelche event (from day 0 to day +1) in all seasons.

Surface circulation during day 0 in summer is characterized by southerlies along the coastal region and the central depression in south-central Chile and easterlies or downslope winds over the western Andean slope,

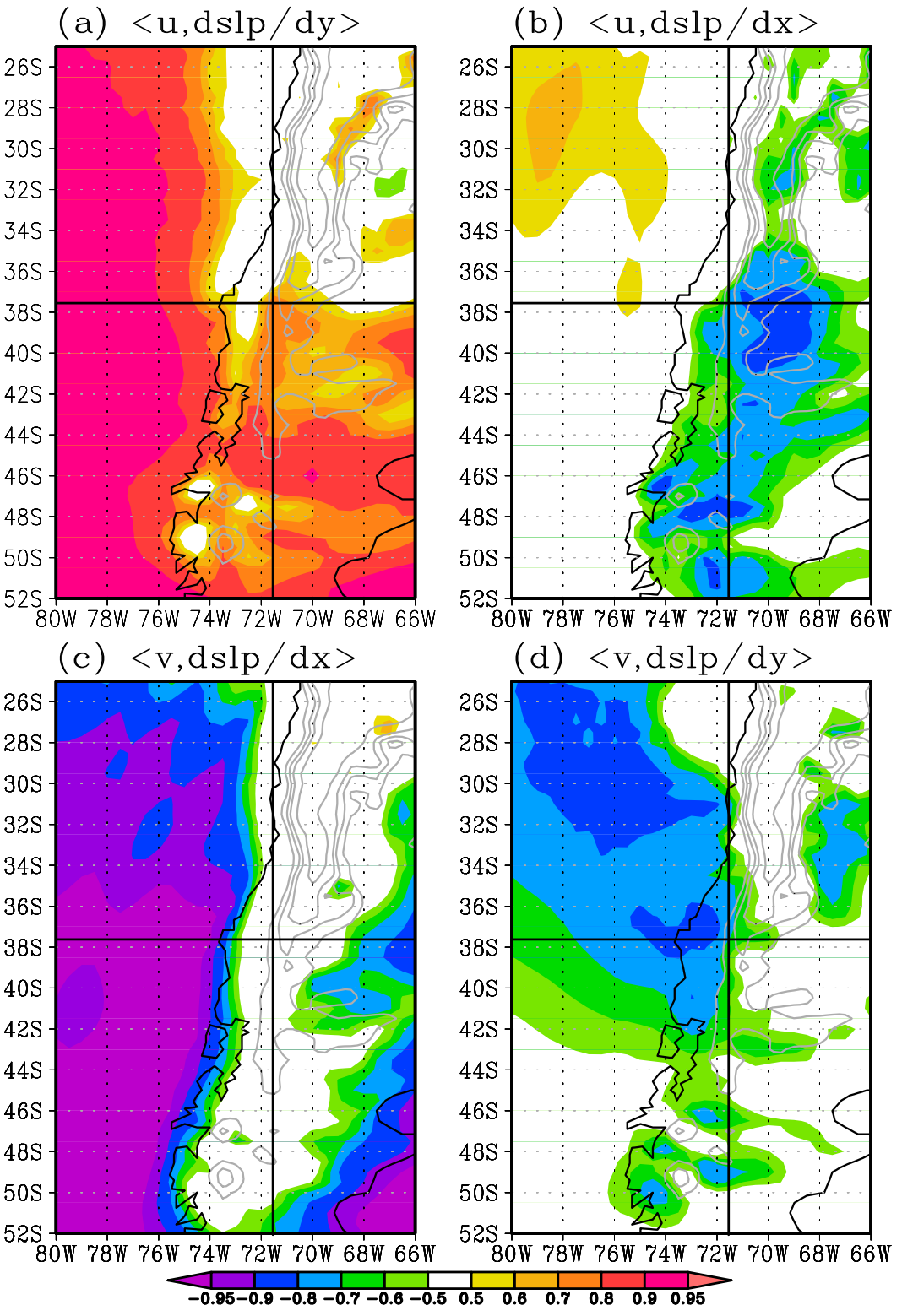

FIG. 7. Point-to-point correlation between CFSR wind components and CFSR SLP gradients based on daily anomalies for the entire period January 1979–February 2015. (a) Zonal wind and meridional SLP gradient, (b) zonal wind and zonal SLP gradient, (c) meridional wind and zonal SLP gradient, and (d) meridional wind and meridional SLP gradient. Correlations are depicted every 0.1. Correlations in the interval from −0.5 to 0.5 are not depicted. Gray contours represent topographic altitude levels of 1000, 1500, 2000, and 3000 m MSL. The intersection of the horizontal and vertical thin black lines in each panel shows the grid point 37.5°S, 71.5°W, used to define Puelche events.

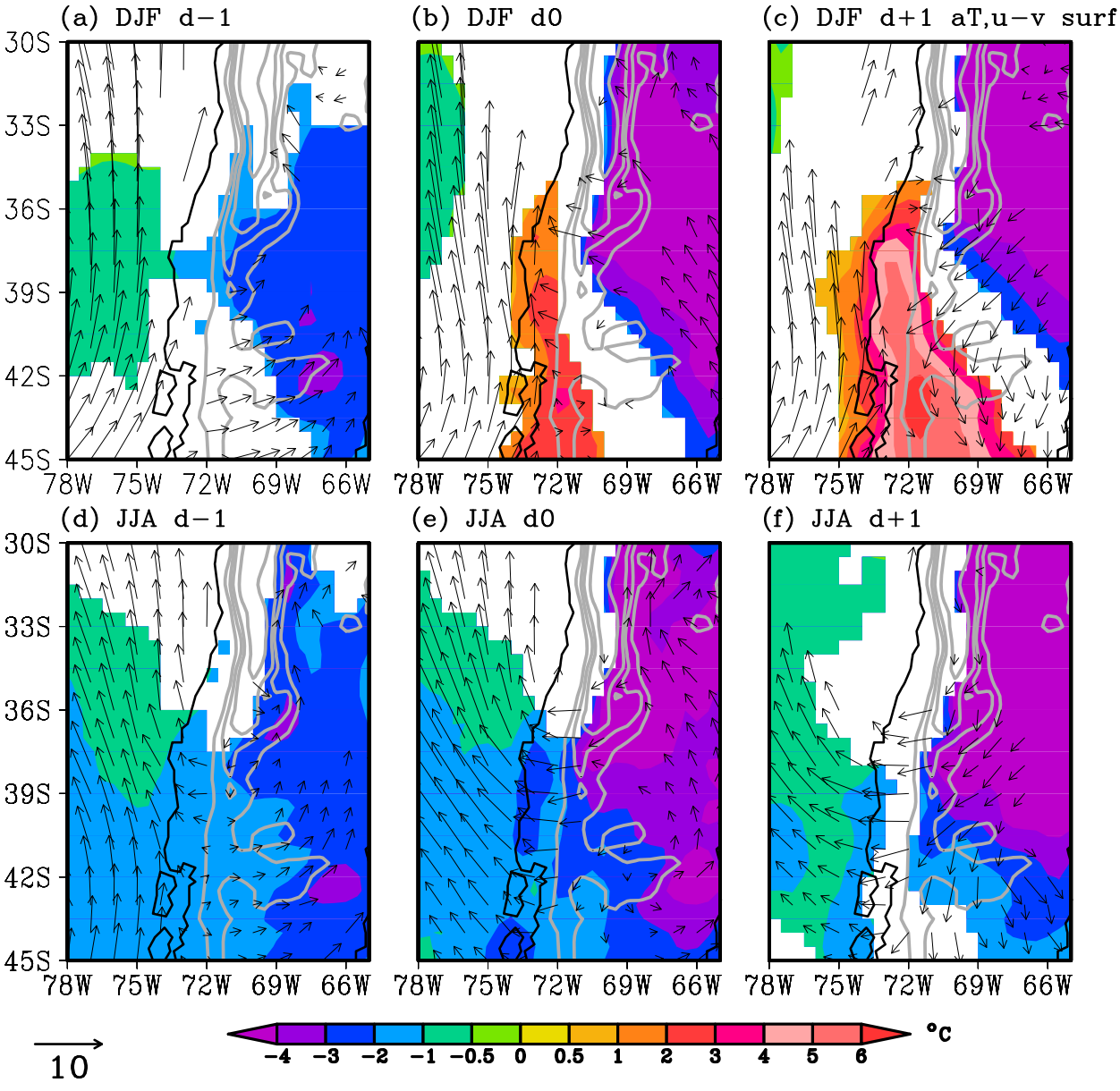

FIG. 8. Composite of the surface CFSR temperature anomalies (°C; color shades) and surface wind ($m\,s^{-1}$; vectors): (a),(d) one day before; (b),(e) the first day of; and (c),(f) the second day of Puelche events that last two days. The composites are shown for summer in (a)–(c) and winter in (d)–(f). Composites are shown when values are significant at 95% of confidence based on a Monte Carlo test. Composite averages are based on absolute wind values, and anomaly values for temperature for the period January 1979–February 2015. Gray contours represent topographic altitude levels of 1000, 1500, 2000, and 3000 m MSL.

including the foothill of the Andes Mountains, in the latitudinal band 36°–40°S (Figs. 8a–c). By day +1 southerly winds are restricted to the coastal ocean while easterlies are still present over the Andes and appear stronger in Argentina. During winter, as for fall and spring (not shown), the surface circulation is slightly different. For day 0, while the easterlies over the western Andean slope in the region 36°–39°S are stronger than during summer, easterlies are observed over the central depression of Chile. At the same time, southeasterlies dominate the oceanic area (Figs. 8d–f). By day +1, this pattern persists in Chile, but northeasterly winds develop in the Argentinian side of the Andes Mountains. In all seasons, the surface circulation during the day prior to the Puelche onset is characterized by southerly winds over the coastal ocean and westerlies over the continent south of 40°S. At 850 hPa (Fig. 9), a very similar but strengthened circulation pattern is observed, although the wind

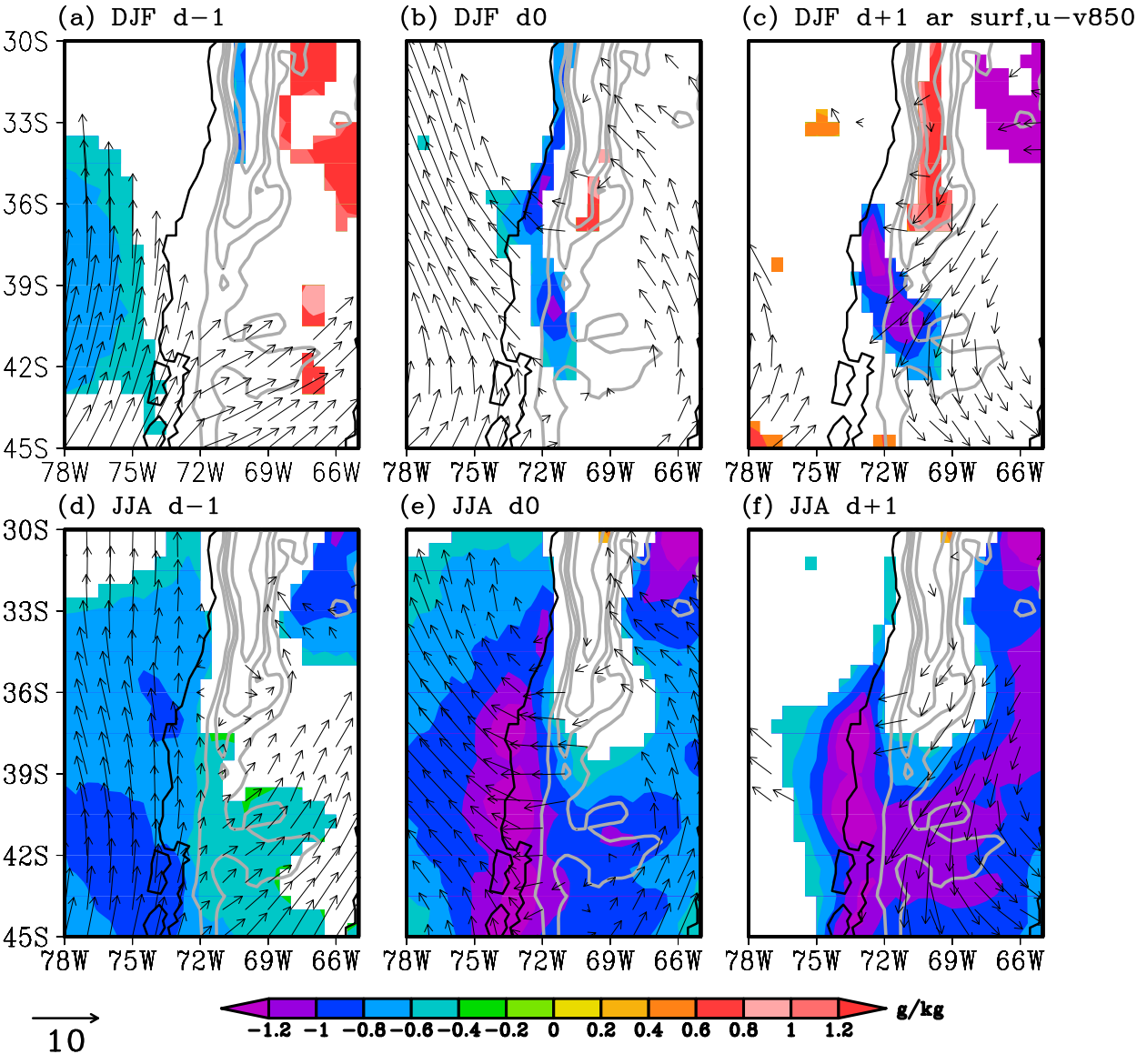

FIG. 9. As in Fig. 8, but for surface CFSR water vapor mixing ratio anomalies (g kg^{-1}; shades) and absolute wind values at 850 hPa (m s^{-1}; vectors).

tends to have a larger negative zonal component to the west of the Andes.

In relation to humidity at the surface (Fig. 9), negative water vapor mixing ratio anomalies dominate most areas over the coastal ocean and south-central Chile and Argentina, from day −1 to day +1. This is particularly manifest in winter (Figs. 9d–f) and spring (not shown). The negative humidity anomalies increase during day 0, showing values lower than −1 g kg^{-1} especially over coastal areas of south-central Chile that also persist during day +1. In summer (Figs. 9a–c) and fall (not shown), negative water vapor mixing ratio anomalies are observed from 33° to 42°S in Chile during day 0. The second day of the Puelche event, the area with negative anomalies decreases, while at the summit of the Andes positive anomalies are present to the north of 37°S.

According to the circulation patterns shown in Figs. 5, 8 and 9, the zonal circulation across the Andes Mountains in the region 36°–40°S is characterized by easterlies with upslope (downslope) winds in the eastern (western) Andean slope. A cross section along 37.5°S shows that the presence of the easterlies during the Puelche episode extends well above the Andes summit until 600 hPa during day 0 (Figs. 10b,e). Away from the summit, to the west and east, the wind direction is mainly southeast. At the surface, easterlies are observed in winter but not in

summer. By day +1, southeasterlies persist over the coastal sea while the eastern flank of the Andes is dominated by strong northeasterlies. Fall and spring show similarities with summer and winter, respectively (not shown). Day −1 is characterized by negative temperature anomalies in sectors to the west and to the east of the Andes (Figs. 10a,d). By day 0, a warming is observed to the west of the Andes summit from 900 to 700 hPa, while negative temperature anomalies are observed to the east from the surface upward. By day +1, the positive temperature anomalies increase, with a clear nucleus at about 900 hPa elongated to the west over the coastal ocean. In Argentina, negative anomalies are observed from the surface up to 800 hPa. Along with the positive temperature anomalies over Chile and the coastal ocean, Fig. 10 also shows the important presence of negative water vapor mixing ratio anomalies on the order of $-1.5\,g\,kg^{-1}$, with a maximum along 900 hPa during day 0 and day +1 of the Puelche event. These anomaly patterns are similar for fall and spring (not shown), with the exception of the positive temperature anomaly, which is only observed during day +1 during both seasons.

Along with the eastward displacement of the migratory high pressure system at the surface, the synoptic-scale subsidence in the region between the midtropospheric trough to the east and the ridge to the west (Figs. 5b,e), would explain the regional pattern of warming and drying of the free atmosphere over south-central Chile (Figs. 8, 9, and 10). The warming aloft would be the result of the adiabatic compression of the air, while the subsidence would advect dry air downward. Remarkably, this warming induced during Puelche episodes has been related to two quite different processes occurring near the volcano and Lake Villarrica, in south-central Chile: glacier melt events during winter (Brock et al. 2012) and increased phytoplanktonic productivity at the end of summer (Meruane et al. 2005). In particular, the glaciers of Villarrica volcano, located at about 39.4°S, 71.9°W with an equilibrium line altitude of 2000 m MSL, experience ablation episodes during winter because of intense warming resulting from adiabatic compression and then to warm advection by the upstream northwesterlies. On the other hand, phytoplanktonic productivity in Lake Villarrica, at about 38.3°S, 72.1°W and 230 m MSL, is increased by vertical mixing forced by strong easterly winds (Meruane et al. 2005). These winds, identified as Puelche, are characterized by increases in temperature and decreases of relative humidity along the entire day.

c. *Local impacts*

The results shown in this work suggest that the easterly flow moving down the western slope of the Andes in south-central Chile does not always reach the surface, especially in summer (Figs. 8 and 10, and observed evidence in Fig. 4). However, strong warming is observed in the region to the west of the Andes over the central depression and coastal areas of south-central Chile. With respect to this, Hoinka (1985) showed that, during foehn and chinook episodes in the Alps and the Rocky Mountains, respectively, the increases in temperature and decreases in relative humidity are detected far from the foothills where strong downslope gusts are present; he named this process foehn clearance. The cloudless sky and drier atmosphere would allow an increase in solar radiation reaching the surface and a subsequent warming of the near-surface air (Hoinka 1985). On the other hand, Zhong et al. (2001) pointed out that under large-scale subsidence, the longwave radiative loss of the surface is enhanced, resulting in a larger cooling during the night. The foehn clearance in south-central Chile is suggested in Fig. 8 by the daily positive temperature anomalies, especially during summer and fall (not shown).

To further investigate the response of temperature, based on AWS data, over the central depression and coastal areas of south-central Chile, when Puelche winds are present in the western Andes slope, the daily cooling and warming were characterized as follows: The difference between the minimum temperature of one day and the maximum temperature of the previous day defines the cooling (°C), while the difference between the maximum and minimum temperatures of the same day defines the warming (°C). The daily cooling and warming was then averaged for the region 35°–40°S using the available weather stations for this study in the period 2009–13 (Fig. 1). In Fig. 11a the composite regional cooling (in absolute values) and warming are shown for two-day Puelche episodes, including the two days prior and after the episodes as well. First of all, the largest cooling and warming (or diurnal temperature amplitude) occur during the dry summer season when the soil has lost humidity, the surface receives more solar radiation, and cloudy conditions are less frequent. Less intense warming and cooling are observed in the other seasons, especially in winter. The warming is clearly enhanced during the two days of Puelche, with a mean increase of temperature of about 20°C in summer and of about 14°–16°C in winter. The cooling during the night by the enhanced radiative loss, suggested by Zhong et al. (2001), is strongest during the days after the onset of the Puelche event (−19°C in summer and −14°C in winter). Interestingly, significant frost episodes in central Chile during winter have been also associated with migratory high pressure systems passing eastward across the Andes (Montes et al. 2013), which is an indication of the foehn clearance also occurring at these lower latitudes.

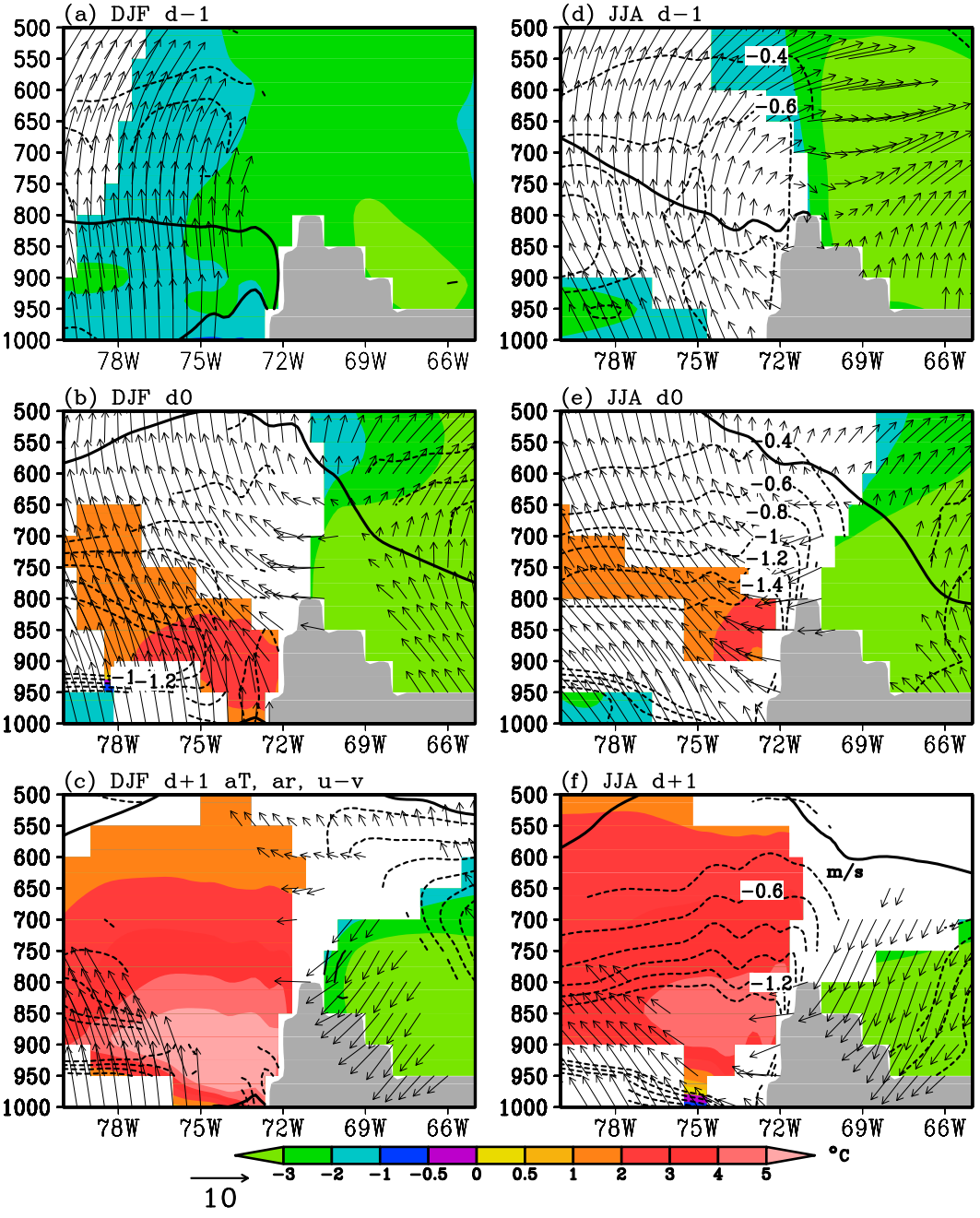

FIG. 10. Longitude–height cross-section composites, at 37.5°S, of horizontal winds ($m\,s^{-1}$; vectors), temperature anomalies (°C; color shades), and water vapor mixing ratio anomalies ($g\,kg^{-1}$; contours): (a),(d) one day before; (b),(e) the first day of; and (c),(f) the second day of Puelche events that last two days. The composites are shown for summer in (a)–(c) and winter in (d)–(f). Composites are shown when values are significant at 95% of confidence based on a Monte Carlo test. Composite averages are based on absolute wind values, and anomaly values for temperature and water vapor mixing ratio in the period January 1979–February 2015. The zero zonal wind speed is depicted with a thick black line. The gray area represents the model topography.

An additional analysis was conducted to verify the role of cloudiness during Puelche events, particularly during the day +1, when daytime warming and nighttime cooling the following morning are significant for both summer and winter. Figures 12a and 12c show the climatology of clear-sky fraction. To the north of 37°S, the amount of clear sky is above 80% during summer, that is, more than 80% of these days (afternoon) are

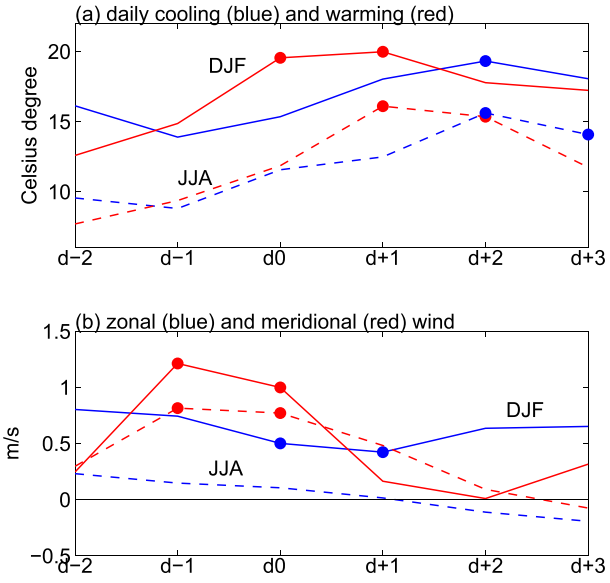

FIG. 11. (a) Composite of the nighttime cooling (blue lines) and diurnal warming (red lines) in degrees Celsius for two days prior to, during, and after the Puelche events for summer (solid lines) and winter (dashed lines) conditions, based on data of AWSs in the central depression with observations in the 2009–13 period (Fig. 1b). (b) As in (a), but for zonal (blue lines) and meridional (red lines) surface winds. See text for definition of nighttime cooling and diurnal warming. Circles indicate significant values at 95% of confidence based on a Monte Carlo test.

characterized by the absence of clouds. South of 37°S the fraction of clear sky decreases down to 50% at 40°S. During winter, to the north of 35°S this fraction is about 50%, decreasing southward to 20% at 40°S. During day +1 of Puelche events, the composite of the clear-sky fraction is over 90% (70%) in the entire study region for summer (winter) (not shown). In accordance with the differences in climatology (Figs. 12b,d), there is an increase in the clear-sky fraction in south-central Chile, which is statistically significant to the south of 37°S. Interestingly, during summer, a large area of the study region shows insignificant increases in the clear-sky fraction. Presumably, Puelche events contribute to the large fraction of clear-sky days observed during summer.

Another well-documented regional-scale weather phenomenon associated with the migratory cold anticyclone is the presence of a southerly low-level jet off central Chile (Garreaud and Muñoz 2005; Muñoz and Garreaud 2005). Because of the presence of the coastal range, the geostrophic wind forced by the reversed meridional pressure gradient is precluded in the marine boundary layer, and therefore geostrophic easterly winds are replaced by alongshore southerly winds accelerated by the high pressure system located to the south (Muñoz and Garreaud 2005). Strong southerly winds are observed consistently off south-central Chile, especially during summer, when a Puelche event develops in the western Andes Mountains (Figs. 8 and 10). Furthermore, southerly winds are also observed in the central depression, between the coast and the Andes. The compositing analysis of the regional surface wind (Fig. 11b), defined by the average of the weather stations located between 35° and 40°S at altitudes lower than 500 m MSL (Fig. 1), confirms the strengthening of southerly winds but also the presence of westerlies or insignificant easterlies. According to this analysis, the alongshore acceleration starts the day before the onset of the Puelche wind when the migratory anticyclone has reached the western coast of the continent. It persists during the first day of the event, but during the second day, when the coastal trough is well developed and located at 35°S, it weakens. It is also confirmed that Puelche winds are not observed, on average, in the central depression during any season.

4. Conclusions

The existence of Puelche winds in Chile, an easterly foehnlike wind descending on the western slope of the Andes Mountains, has been known by the meteorological community at least since the mid-twentieth century. However, to our knowledge, this is the first time a climatological characterization of the Puelche wind in south-central Chile has been accomplished. The analysis is based on the CFSR–NCEP reanalyzed data, validated by surface weather observations. To describe the synoptic forcing of Puelche, the development of the near-surface circulation, and the associated temperature and humidity anomalies at regional scale, a compositing analysis is performed.

The main synoptic-scale forcing of Puelche winds in south-central Chile is the passage of cold anticyclonic systems across the Andes Mountains (between Chile and Argentina). As the midlatitude high pressure system progresses into the South American continent, there is an acceleration of southerly winds near the surface from the Andes foothills to the coastal ocean off south-central Chile, while an east-to-west circulation is established over the Andes Mountains. The Puelche winds rarely reach the surface to the west of the Andes foothills, over the central depression and the coastal plain. Also, the synoptic-scale subsidence between the midtropospheric trough to the east and the ridge to the west would explain the regional pattern of warming and drying of the free atmosphere over south-central Chile, whose nucleus is located at 900 hPa.

As in other places where foehnlike winds develop, the warming extends far from places where the Puelche is

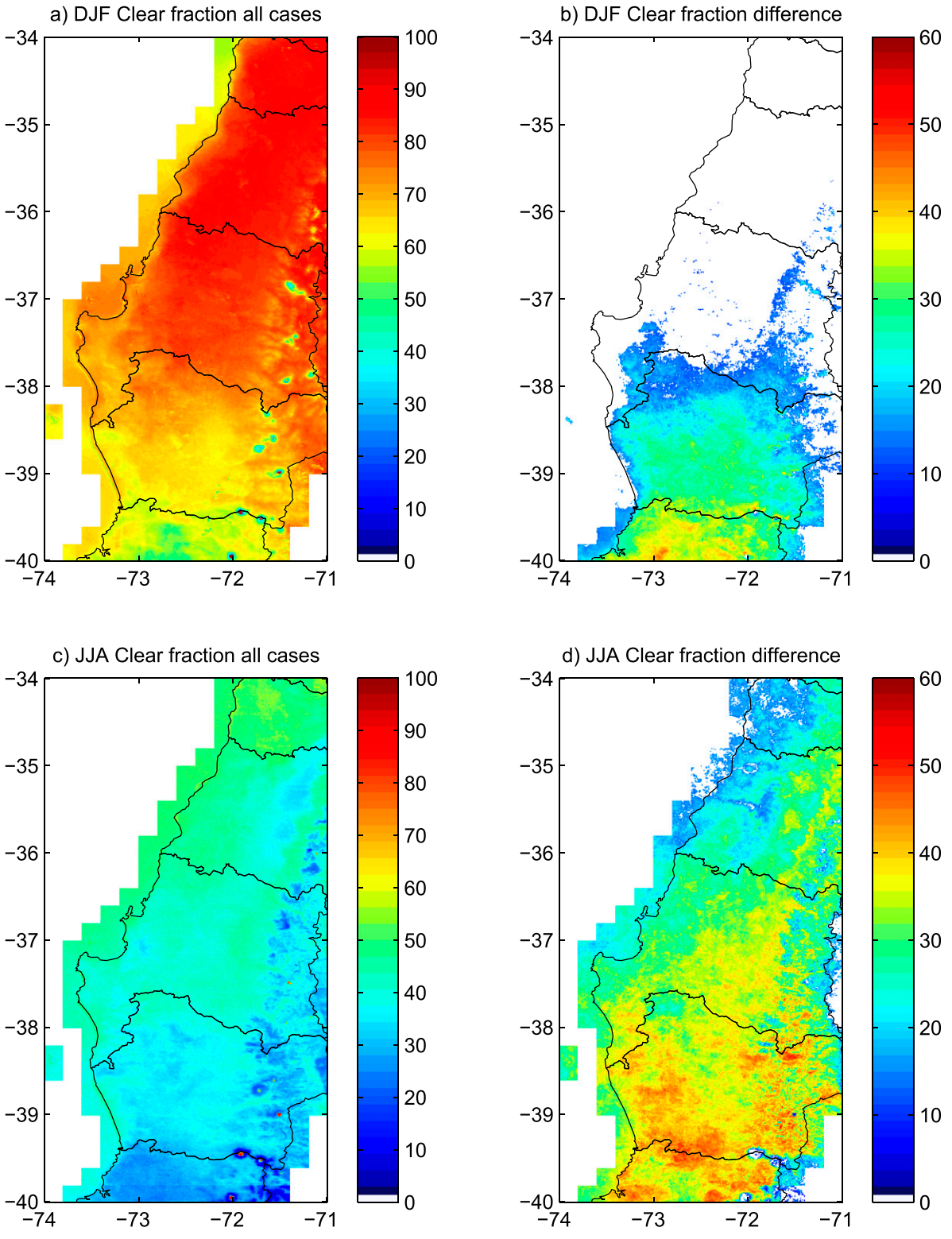

FIG. 12. Impact of Puelche events on cloud coverage based on GOES visible imagery for the period 2004–14 at 0900, 1200, and 1500 UTC. (a) Average clear fraction for summer (%). (b) Clear fraction of summer Puelche events (%) at day +1 minus the average clear fraction (only differences with significance > 95% are shown, based on a Monte Carlo test). (c) As in (a), but for winter. (d) As in (b), but for winter Puelche events.

actually observed, that is, at the surface in coastal areas and the central depression. This foehn clearance is the result of cloudless sky and drier atmosphere that would allow an increase in solar radiation reaching the surface and a subsequent warming of the near-surface air. The foehn clearance also drives an enhanced nighttime cooling especially in the second day of an event and the day after.

The mean meridional scale of Puelche winds is about 600 km, covering the latitudinal band of 35°–40°S during summer, but extending to 45°S during fall, winter, and spring, although with smaller easterly speeds to the south of 43°S. Thus, the occurrence of Puelche winds in south-central Chile is not related to the occurrence of downslope Andean winds in central Chile (terral at ~30°S and raco at ~33°S). The results shown here suggest that an important factor is the latitudinal position of the migratory anticyclone crossing the continent. When the high pressure center moves eastward along 50°S (40°S), downslope winds are forced in south-central (central) Chile. It is also suggested that the altitude of the Andes Mountains plays a key role in the differentiation of the occurrence and behavior of downslope winds in its western slope. To the north of 35°S the Andes height is over 4000 m MSL, while to the south it drops reaching 2000 m MSL at 37°. This meridional elevation gradient appears to be responsible of two notable differences between terral/raco and Puelche winds. The terral and raco winds are not linked with upslope movement in the Argentinian slope of the Andes and it is geostrophically forced by meridional pressure gradients. However, the Puelche wind is part of a zonal circulation from Argentina (upslope) to Chile (downslope), which is forced by both meridional and zonal pressure gradients.

Acknowledgments. The authors thank three anonymous reviewers for their helpful comments and suggestions to the original manuscript. This work was supported by Comisión Nacional de Investigación Científica y Tecnológica (CONICYT) Chile through Grant Fondecyt 1131092. The corresponding author was partially supported by CHRIAM/CONICYT/FONDAP-15130015. CFSR–NCEP reanalysis data were provided by the Research Data Archive maintained by the Computational and Information Systems Laboratory at NCEP. Meteorological and radiosonde data were supplied by the Chilean National Weather Service (DMC) and also by the Bureau of Water Management (DGA-MOP), the Fruit Development Foundation (FDF), the Agricultural Research Institute (INIA), and COLBUN S.A. Most figures were produced with the Grid Analysis and Display System (GrADS).

REFERENCES

Barry, R. G., 2008: *Mountain Weather and Climate*. 3rd ed. Cambridge University Press, 512 pp.

Brinkmann, W. A., 1971: What is a foehn? *Weather*, **26**, 230–239, doi:10.1002/j.1477-8696.1971.tb04200.x.

Brock, B. W., F. Burger, A. Rivera, and A. Montecinos, 2012: A fifty year record of winter glacier melt events in southern Chile, 38°–42°S. *Environ. Res. Lett.*, **7**, 045403, doi:10.1088/1748-9326/7/4/045403.

Chawla, A., D. M. Spindler, and H. L. Tolman, 2013: Validation of a thirty year wave hindcast using the Climate Forecast System Reanalysis winds. *Ocean Modell.*, **70**, 189–206, doi:10.1016/j.ocemod.2012.07.005.

Drechsel, S., and G. J. Mayr, 2008: Objective forecasting of foehn winds for a subgrid-scale Alpine valley. *Wea. Forecasting*, **23**, 205–218, doi:10.1175/2007WAF2006021.1.

Fuenzalida, H., 1982: A country of climate extremes (in Spanish). *Chile: Essence and Evolution*, H. García, Ed., Universidad de Chile, Santiago, 27–35.

Gaffin, D. M., 2007: Foehn winds that produced large temperature differences near the southern Appalachian Mountains. *Wea. Forecasting*, **22**, 145–159, doi:10.1175/WAF970.1.

Garreaud, R., and J. Rutllant, 2003: Coastal lows in north-central Chile: Numerical simulation of a typical case. *Mon. Wea. Rev.*, **131**, 891–908, doi:10.1175/1520-0493(2003)131<0891:CLATSW>2.0.CO;2.

——, and R. Muñoz, 2005: The low-level jet off the subtropical west coast of South America: Structure and variability. *Mon. Wea. Rev.*, **133**, 2246–2261, doi:10.1175/MWR2972.1.

——, and M. Falvey, 2009: The coastal winds off western subtropical South America in future climate scenarios. *Int. J. Climatol.*, **29**, 543–554, doi:10.1002/joc.1716.

——, J. Rutllant, and H. Fuenzalida, 2002: Coastal lows in north-central Chile: Mean structure and evolution. *Mon. Wea. Rev.*, **130**, 75–88, doi:10.1175/1520-0493(2002)130<0075:CLATSW>2.0.CO;2.

Glenn, C. L., 1961: The chinook. *Weatherwise*, **14**, 175–182, doi:10.1080/00431672.1961.9930019.

Hoinka, K. P., 1985: What is a foehn clearance? *Bull. Amer. Meteor. Soc.*, **66**, 1123–1132, doi:10.1175/1520-0477(1985)066<1123:WIAFC>2.0.CO;2.

Markowski, P. M., and Y. P. Richardson, 2010: *Mesoscale Meteorology in Midlatitudes*. Wiley-Blackwell, 407 pp.

McGowan, H. A., and A. P. Sturman, 1996: Regional and local scale characteristics of foehn wind events over the South Island of New Zealand. *Meteor. Atmos. Phys.*, **58**, 151–164, doi:10.1007/BF01027562.

Meruane, C., Y. Niño, and R. Garreaud, 2005: Simulation of phytoplankton response to strong wind events in lake Villarrica, Chile. *XXXI IAHR Congress*, Seoul, South Korea, International Association of Hydraulic Engineering, doi:10.13140/RG.2.1.2848.8403.

Molina, A., 2012: A semi-empirical model for surface solar radiation in Chile (in Spanish). M.S. thesis, Department of Geophysics, University of Chile, 32 pp.

Montecinos, A., and F. Gomez, 2010: ENSO modulation of the upwelling season off southern-central Chile. *Geophys. Res. Lett.*, **37**, L02708, doi:10.1029/2009GL041739.

Montes, C., R. Muñoz, and J. Perez-Quezada, 2013: Surface atmospheric circulation patterns and associated minimum temperatures in the Maipo and Casablanca valleys, central Chile. *Theor. Appl. Climatol.*, **111**, 275–284, doi:10.1007/s00704-012-0663-5.

——, J. Rutllant, A. Aguirre, L. Bascuñán-Godoy, and C. Juliá, 2016: Terral de Vicuña, a foehnlike wind in semiarid northern Chile: Meteorological aspects and implications for the fulfillment of chill requirements in deciduous fruit trees. *J. Appl. Meteor. Climatol.*, **55**, 1183–1195, doi:10.1175/JAMC-D-15-0275.1.

Muñoz, R., and R. Garreaud, 2005: Dynamics of the low-level jet off the subtropical west coast of South America. *Mon. Wea. Rev.*, **133**, 3661–3677, doi:10.1175/MWR3074.1.

Norte, F. A., 1988: Zonda wind characteristics in the region of Cuyo (in Spanish). Ph.D. thesis, Buenos Aires University, 255 pp.

——, 2015: Understanding and forecasting zonda wind (Andean foehn) in Argentina: A review. *Atmos. Climate Sci.*, **5**, 163–193, doi:10.4236/acs.2015.53012.

——, A. G. Ulke, S. C. Simonelli, and M. Viale, 2008: The severe zonda wind event of 11 July 2006 east of the Andes Cordillera (Argentine): A case study using the BRAMS model. *Meteor. Atmos. Phys.*, **102**, 1–14, doi:10.1007/s00703-008-0011-6.

Plavcan, D., G. J. Mayr, and A. Zeileis, 2014: Automatic and probabilistic foehn diagnosis with a statistical mixture model. *J. Appl. Meteor. Climatol.*, **53**, 652–659, doi:10.1175/JAMC-D-13-0267.1.

Quaile, E. L., 2001: Back to basics: Foehn and chinook winds. *Weather*, **56**, 141–145, doi:10.1002/j.1477-8696.2001.tb06551.x.

Rahn, D. A., and R. Garreaud, 2014: A synoptic climatology of the near-surface wind along the west coast of South America. *Int. J. Climatol.*, **34**, 780–792, doi:10.1002/joc.3724.

Raphael, M. N., 2003: The Santa Ana winds of California. *Earth Interact.*, **7**, doi:10.1175/1087-3562(2003)007<0001:TSAWOC>2.0.CO;2.

Rimac, A., J. S. von Storch, C. Eden, and H. Haak, 2013: The influence of high-resolution wind stress field on the power input to near-inertial motions in the ocean. *Geophys. Res. Lett.*, **40**, 4882–4886, doi:10.1002/grl.50929.

Rondanelli, R., A. Molina, and M. Falvey, 2015: The Atacama surface solar maximum. *Bull. Amer. Meteor. Soc.*, **96**, 405–418, doi:10.1175/BAMS-D-13-00175.1.

Rutllant, J., and R. Garreaud, 1995: Meteorological air pollution potential for Santiago, Chile: Towards an objective episode forecasting. *Environ. Monit. Assess.*, **34**, 223–244, doi:10.1007/BF00554796.

——, and ——, 2004: Episodes of strong flow down the western slope of the subtropical Andes. *Mon. Wea. Rev.*, **132**, 611–622, doi:10.1175/1520-0493(2004)132<0611:EOSFDT>2.0.CO;2.

——, B. Rosenbluth, and S. Hormazabal, 2004: Intraseasonal variability of wind-forced coastal upwelling off central Chile (30° S). *Cont. Shelf Res.*, **24**, 789–804, doi:10.1016/j.csr.2004.02.004.

Saha, S., and Coauthors, 2010: The NCEP Climate Forecast System Reanalysis. *Bull. Amer. Meteor. Soc.*, **91**, 1015–1057, doi:10.1175/2010BAMS3001.1.

——, and Coauthors, 2014: The NCEP Climate Forecast System version 2. *J. Climate*, **27**, 2185–2208, doi:10.1175/JCLI-D-12-00823.1.

Seluchi, M., F. A. Norte, P. Satyamurty, and S. Chan-Chou, 2003: Analysis of three situations of the foehn effect over the Andes (zonda wind) using the Eta–CPTEC regional model. *Wea. Forecasting*, **18**, 481–501, doi:10.1175/1520-0434(2003)18<481:AOTSOT>2.0.CO;2.

Stopa, J. E., and K. F. Cheung, 2014: Intercomparison of wind and wave data from the ECMWF Reanalysis Interim and the NCEP Climate Forecast System Reanalysis. *Ocean Modell.*, **75**, 65–83, doi:10.1016/j.ocemod.2013.12.006.

Strub, P. T., J. M. Mesias, V. Montecino, J. Rutllant, and S. Salinas, 1998: Coastal ocean circulation off western South America. *The Global Coastal Ocean: Processes and Methods*, A. R. Robinson and K. H. Brink, Eds., *The Sea—Ideas and Observations on Progress in the Study of the Seas*, Vol. 10, John Wiley and Sons, 273–313.

Sturman, A. P., 1987: Thermal influences on airflow in mountainous terrain. *Prog. Phys. Geogr.*, **11**, 183–206, doi:10.1177/030913338701100202.

von Storch, H., and F. W. Zwiers, 1999: *Statistical Analysis in Climate Research*. Cambridge University Press, 484 pp.

Whiteman, C. D., 2000: *Mountain Meteorology: Fundamentals and Applications*. Oxford University Press, 355 pp.

——, and J. C. Doran, 1993: The relationship between overlying synoptic-scale flows and winds within a valley. *J. Appl. Meteor.*, **32**, 1669–1682, doi:10.1175/1520-0450(1993)032<1669:TRBOSS>2.0.CO;2.

WMO, 1992: *International Meteorological Vocabulary*. 2nd ed. Vol. 182, World Meteorological Organization, 784 pp.

Yu, L., S. Zhong, X. Bian, and W. E. Heilman, 2016: Climatology and trend of wind power resources in China and its surrounding regions: A revisit using Climate Forecast System Reanalysis data. *Int. J. Climatol.*, **36**, 2173–2188, doi:10.1002/joc.4485.

Zhang, H., and J. Sheng, 2013: Estimation of extreme sea levels over the eastern continental shelf of North America. *J. Geophys. Res.*, **118**, 6253–6273, doi:10.1002/2013JC009160.

Zhong, S., C. D. Whiteman, X. Bian, W. J. Shaw, and J. M. Hubbe, 2001: Meteorological processes affecting the evolution of a wintertime cold air pool in the Columbia basin. *Mon. Wea. Rev.*, **129**, 2600–2613, doi:10.1175/1520-0493(2001)129<2600:MPATEO>2.0.CO;2.